BEAM ENERGY MANAGEMENT AND RF FAILURE COMPENSATION SCENARIOS FOR THE EUROPEAN XFEL

Bolko Beutner, DESY, Hamburg, Germany

Abstract

Total beam delivery time to user stations is a key parameter for FEL user facilities. Therefore downtime due to RF issues, among other things, should be minimized. Specifically in case of a RF failure machine operation and beam delivery should be maintained as long as the next scheduled maintainance day. This is achieved by increasing the power in all remaining klystrons to recover the lost beam energy. These modification of the beam energy profile along the machine induces an optics perturbation which is typically compensated by a rescaling of the quadrupole magnet gradients to maintain a constant focusing strength. However, we would like to resume operation at the next macro-pulse after a RF event. While, in general, the RF systems can handle such changes the magnets can not. In this paper we will explore optics perturbations for the case that we do not change the magnets at all, to estimate the feasibility of fast beam recovery after klystron failure. In addition corrections to the RF setup are calculated with the goal of avoiding changes in the bunch compression dynamics of the machine.

BEAM ENERGY MANAGEMENT FOR THE EUROPEAN XFEL

Superconducting technology used at the European XFEL allows for RF pulses as long as 600 μs supporting bunch trains with an internal repetition rate of up to 4.5 MHz. These pulses are, which are refereed to as *macro-pulses* are triggered with 10 Hz. The European XFEL is driven in total by 26 1.3 GHz multi-beam klystrons [1] [2]. These RF stations are distributed along European XFEL as shown in Fig. 1.

The energy gain ΔE, number of RF stations N, and individual voltages per klystron $\Delta E/N$ and cavity V are summarized in Table 1. Each klystron in the Linac 1-3 sections drives four accelerator cryo-modules consisting of eight cavities with a total energy gain up to 755 MeV. Design gradient of the niobium cavities is 23.6 MV/m. Since the assembly of the cryo-modules is work in progress we do not have final numbers on the actual available gradient. After final testing and should the situation arise re-treatment of all modules we assume an available gradient of 23.6 MV/m with an average overhead of 10% [3]. Linac 3 is configured to achieve nominal final beam energy of 17.5 GeV at the nominal gradient of 23.6 MV/m using 20 instead of 21 RF stations as beam energy reserve.

In the following the name *klystron* refers to the full RF station including modulator, pulse cables, pulse transformers, klystrons, waveguides, down to the cavities, and failures in each of these components are refereed to as *klystron failure*.

From the point-of-view of electron beam energy management the machine is conveniently separated into three parts. First the Injector and Linac 1 section. In this region of the machine each section is essentially driven by one klystron. Klystron failures in this part are fatal and can not be compensated, immediate repair is required to resume operation. The second part is Linac 2. A reduction of acceleration voltage can be recovered by reserves in Linac 3. This Linac 2 however is upstream of the last bunch compressor chicane. Voltage changes effectively modify the energy chirp at BC2 and therefore the final longitudinal beam profile. In addition to energy profile reorganization the off-crest phases needs modification to maintain the final current profile. Linac 3, the main linac, is the last part. Here the majority of the beam energy is generated and here beam energy variations are corrected. The nominal energy gain of Linac 3 is 15.1 GeV. Since we only rely on 20 instead of 21 klystron stations and assume an 10% energy overhead the total voltage capacity of Linac 3 is 17.4 GeV . This additional energy reserve of about 2.3 GeV can be used to compensate the outage of about three klystron stations.

Table 1: XFEL Energy Gain Configuration

Linac Section	ΔE [GeV]	N	$\Delta E/N$ [MeV]	V [MV/m]
Injector	0.13	1	130	16.5
Linac 1	0.57	1	570	17.8
Linac 2	1.7	3	567	17.7
Linac 3	15.1	21/20	719/755	22.5/23.6

MAIN LINAC ENERGY MANAGEMENT

To redistribute the energy gain along we propose an iterative procedure. We start with an index set I which includes all klystrons used for energy correction. Typically I contains all stations except the failed one. The voltages of modules not in I $\Delta V_{j\notin I}$ are not necessarily set to zero, to allow modeling of reduced gradients in individual stations, e.g. detuned cavities within a module or reduced voltage operations as quench prevention. The voltage of each module in operation is modified according to:

$$\Delta V_i' = \frac{E_{\text{nominal}} - \sum_{j\notin I} \Delta V_j}{|I|} \frac{w_i}{\langle w_i \rangle}, i \in I. \qquad (1)$$

The positive weight factors w_i are chosen to set priorities according to the performance and reliability of the individual RF stations. After voltage scaling according to Eq. 1 each ΔV_i is compared with the individual maximum. If the maximum is exceeded it is set to this maximum and the station

ISBN 978-3-95450-133-5

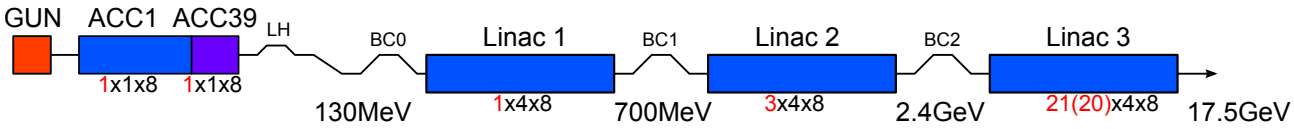

Figure 1: Overview of the XFEL linac and bunch compressor sections. The beam energy at different positions along the machine is given together with the number of RF stations per linac section. For instance Linac 2 consists of 3 klystrons driving 4 modules each containing 8 cavities. Linac 3 is consists of 21 klystron stations.

removed from the set I to have these stations not modified in further iterations. Such iterations continue until the nominal energy gain is retained or all available structures are set to maximum voltage. Examples of such energy profile corrections are shown in Fig. 2, 3, and 4. As mentioned earlier

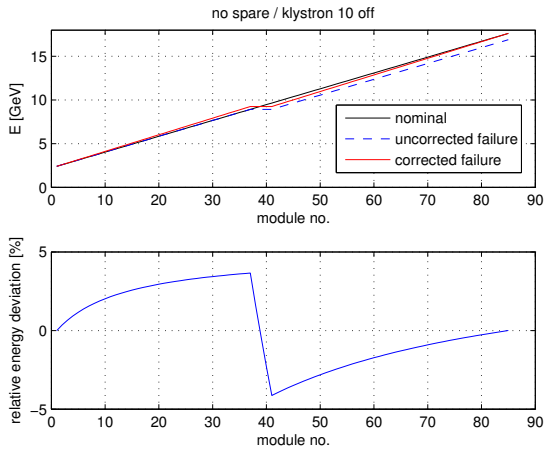

Figure 2: Example of energy correction in Linac 3 of XFEL. In the upper plot the nominal energy profile (black solid), reduced energy after RF failure in station 10 (blue dashed), and the corrected energy profile (red solid) are shown. The relative deviation, the corresponding quadrupole field deviation, along the linac indicated by the module number is shown in the lower plot. In this example no dedicated spare is used, all cavities nominally are operated at 23.6 MV/m · 20/21 =22.5 MV/m.

the main linac is driven by 21 RF stations while only 20 are required for nominal operation. Basically two options can be considered to use this reserve, either all stations are operated at 20/21 of the nominal gradient or one RF stations is not used in nominal operation and activated as needed. In the latter case this "spare" can be located at different positions along the linac.

In the following we consider four scenarios, all stations are in operation, the most downstream station, the middle station or the klystron in the beginning of the main linac are deactivated. Comparing this first two options in Fig. 2 and Fig. 3 we see that in the first case we have an energy deviation at all positions while in the second case the deviation is somewhat localized.

The exact shape of the energy deviation depends on the position of the broken RF station. An overview of the energy

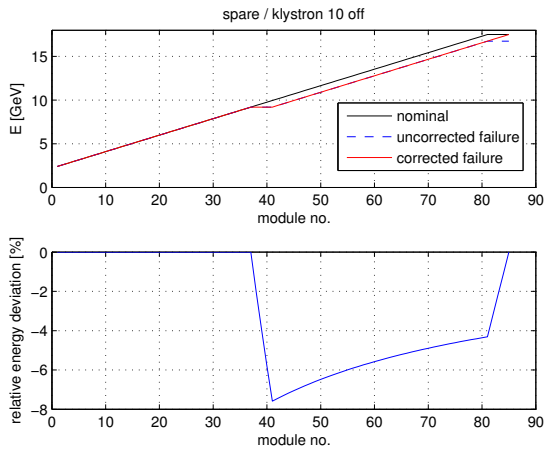

Figure 3: As in Fig. 2. In this example a reserve klystron station is located at the end of the main linac.

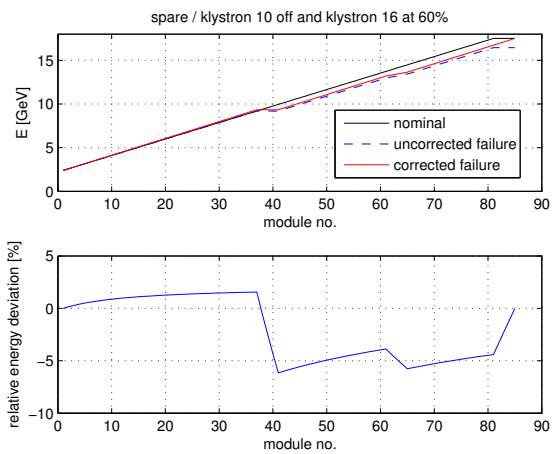

Figure 4: As in Fig. 3. In this example RF station 10 is off and station 16 is set to 60% of nominal gradient.

deviations along the linac for the different scenarios is given in Fig. 5.

The impact on the beam optics mismatch amplitude BMAG $= \xi + \sqrt{\xi^2 - 1}$ with $\xi = 1/2 \cdot (\beta\gamma_0 - 2\alpha\alpha_0 + \gamma\beta_0)$ at the end of the linac with respect to the deign optics is summarized in Fig. 6.

Overall optics mismatch amplitude is optimized in the case with all klystrons in operation and the "spare in the middle" case. In all these situations the maximum deviation from the design optics occurs if the first RF station is out of operation. In general this behavior is expected. As shown

ISBN 978-3-95450-133-5

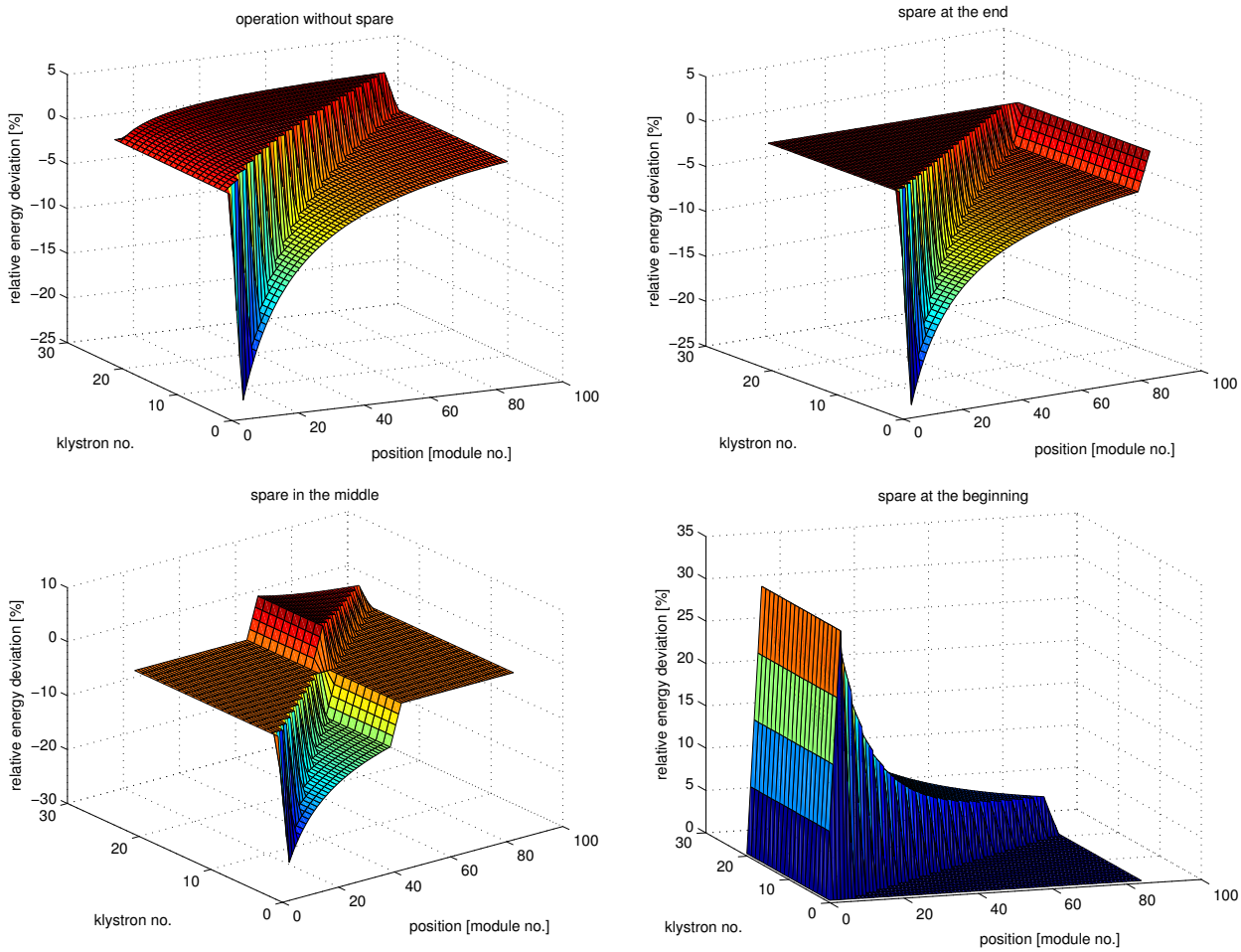

Figure 5: A summary of the energy deviations caused by module failures is shown here. Each plot contains the energy deviation as in the lower plot of Fig. 2 as a function of the klystron which is assumed to be not operational. Different spare scenarios are compared. No dedicated spare is used in the upper left plot. In the remaining scenarios the spare position is at the end, in the middle, or at the beginning of the linac.

ISBN 978-3-95450-133-5

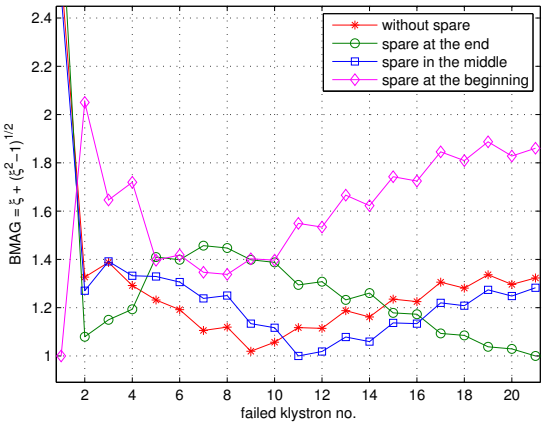

Figure 6: Summary of the optics impact of the different spare scenarios. The optics mismatch at the end of Linac 3 with respect to the nominal optics is plotted vs. the position of a non-operating klystron. In all scenarios excluding the spare at the beginning case the optics deviation caused by the first RF stations in the linac are as high as BMAG = 2.9.

in Fig. 3 the range in which the quadrupole are "detuned" depends on the distance between the broken Klystron and the average position of the reserve. While the impact on the relative energy deviation is obviously lower at higher energies. Studies on operation with simultaneous operation at different bunch charges indicate that a BMAG of about 1.9 ($\xi = 1.2$) is tolerable [4]. However further studies are required on the effects from this optics mismatch on the FEL performance.

I would conclude that all stations should be in operation all the time with reduced gradient. This optimizes robustness of the beam optics and is, in routine operation, less demanding because of the lower gradient.

BUNCH COMPRESSOR LINAC

Above we discussed energy management in Linac 3 of the European XFEL. In Linac 2 we face a different situation. The relative impact of a RF station is larger due to the lower number of independent RF stations, 3 compared to 21. Therefore the energy of BC2 can not be maintained if a RF station is not operational, which calls for a rescaling of the magnets in BC2 inhibiting fast recovery at the next macropulse. Final energy is corrected in Linac 3 as described in the last section. In addition any change in the acceleration upstream of BC2 affects the energy chirp and thus the compression. One way to treat this problem would be a complete redesign of the longitudinal dynamics of XFEL for different energies at BC2 covering reasonable situations. Such a design strategy is covered in [5], but beyond the scope of this paper.

If only Linac 2 is affected we can find a corrected RF phase which compensates the compression analytically. Two effects play a role here. First of all the voltage changes so the generated energy chirp is affected and has to be corrected by a phase offset. And since the relative energy chirp is relevant for compression the beam energy at BC2 E_{BC}, which is affected by the Linac 2 phase, has to be taken into account as well.

The energy at the chicane E_{BC} reads

$$E_{\mathrm{BC}} = E_0 + eV\cos(\varphi) \tag{2}$$

with the initial energy E_0 at the beginning of Linac 2 section and the voltage V of Linac 2.

For the energy along the bunch at position s holds

$$\begin{aligned} E(s) &= eV\cos\left(\varphi + \frac{2\pi}{\lambda}s\right) + E_0 && (3)\\ &= E_0 + eV\left(\cos(\varphi) - \frac{2\pi}{\lambda}\sin(\varphi)s + \cdots\right) && (4)\\ &\approx E_{\mathrm{BC}} + As, && (5) \end{aligned}$$

with an linear energy chirp $A = -2\pi eV\sin(\varphi)/\lambda$. If we assume that the initial acceleration upstream to E_0 is not on-crest an additional initial chirp term $A_0 s$ has to be added to Eq. 5.

The normalized relative energy deviation $\delta = \frac{E(s)-E(0)}{E(0)} = \frac{A_0 s + As}{E_{\mathrm{BC}}}$ at the bunch compressor is required to be constant to maintain the compression. Therefore

$$\begin{aligned} \frac{A_0 s + As}{E_{\mathrm{BC}}} &= \frac{A_0 s + A' s}{E'_{\mathrm{BC}}} && (6)\\ \frac{A_0 + A}{E_{\mathrm{BC}}} &= \frac{A_0 + A'}{E'_{\mathrm{BC}}} && (7)\\ \frac{A_0 - \frac{2\pi eV}{\lambda}\sin(\varphi)}{E} &= \frac{A_0 - \frac{2\pi eV'}{\lambda}\sin(\varphi')}{E'} && (8)\\ \frac{A_0 - \frac{2\pi eV}{\lambda}\sin(\varphi)}{E_0 + eV\cos(\varphi)} &= \frac{A_0 - \frac{2\pi eV'}{\lambda}\sin(\varphi')}{E_0 + eV'\cos(\varphi')} && (9)\\ a &= \frac{A_0 - \frac{2\pi eV'}{\lambda}\sin(\varphi')}{E_0 + eV'\cos(\varphi')} && (10)\\ a\left(E_0 + eV'\cos(\varphi')\right) &= A_0 - \frac{2\pi eV'}{\lambda}\sin(\varphi') && (11) \end{aligned}$$

with the initial chirp A_0, additional chirp generated in a downstream linac section A, and a convenient constant a defines the corrected phase φ' for a given modified voltage V'. For convenience V' is scaled with a linear energy factor from V. An energy factor of 1 would be nominal operation while 2/3 corresponds to operation with one klystron out of operation in Linac 2 of XFEL.

In the following example we apply Eq. 11 on the 250 pC case of European XFEL with a peak current of 5 kA. It is convenient to solve Eq. 11 numerically which is illustrated in Fig. 7.

The corrected phase φ' and the resulting energy at BC2 E_{BC} are plotted in Fig. 8 and Fig. 9 respectively. Due to this phase changes the energy at BC2 does not scale linearly with the voltage in Linac 2. Especially in the case of reduced Linac 2 voltage we actually lose less energy than expected.

ISBN 978-3-95450-133-5

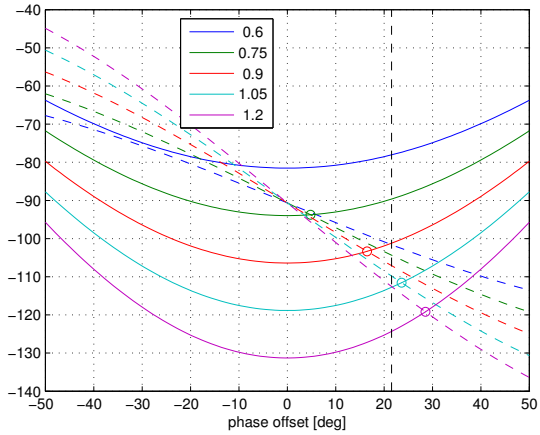

Figure 7: An example of a numerical solution of Eq. 11. The l.h.s (solid lines) and the r.h.s of Eq. 11 (dashed lines) are shown over a range of possible phases φ'. The intersections (circles) indicating the solutions for φ' for different energy factors indicated by a color code. The nominal phase φ (energy factor 1) is indicated by the dashed black vertical line. The case 0.6 has no solution.

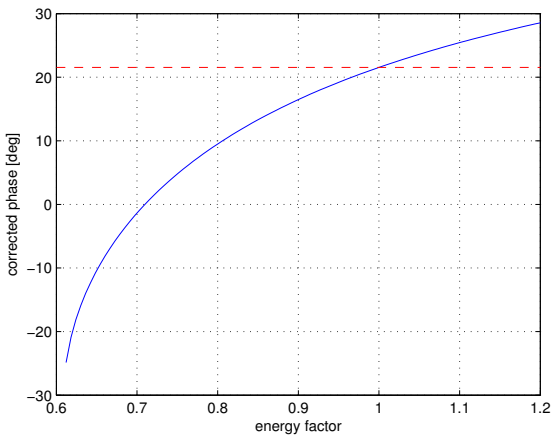

Figure 8: Solution for φ' of Eq. 11. The nominal phase φ (energy factor 1) is indicated by the dashed red line.

Please note that below an energy factor of about 0.61 no solution can be found. Outside of the presented analysis this can be avoided by either a modified R_{56} of the chicane or an upstream modification of the energy chirp A_0.

These solutions are used in numerical simulations of the longitudinal dynamics done with *RF Tweak 5* [6]. The results of these calculations Fig. 10 confirm the validity of Eq. 11. Minor differences in the current profiles can be attributed to self-field effects which depend on the beam energy and are not covered by Eq. 11. Slow beam-based feedback systems which are anyhow foreseen to stabilize the peak current will correct for these effects.

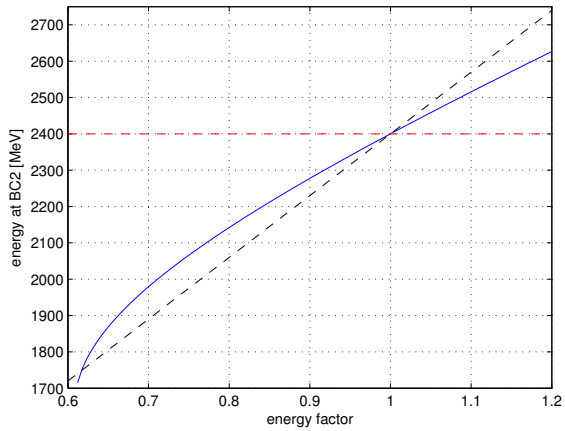

Figure 9: Energy at BC2 E'_{BC} after phase correction is applied. Energy scaled with the energy factor is indicated by the black dashed line. The nominal energy E_{BC} (energy factor 1) is indicated by the dashed red line.

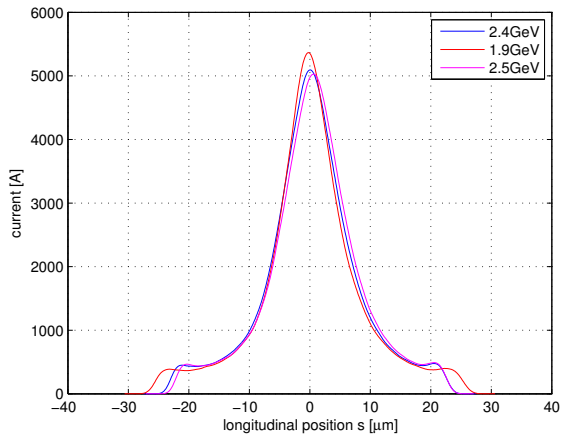

Figure 10: Longitudinal current profiles for different operation points using V' and φ' in Linac 2. The nominal current profile (BC2 at 2.4 GeV) is compared to operation with one klystron less (BC2 at 1.9 GeV) and 10% more energy (BC2 at 2.5 GeV).

CONCLUSION AND OUTLOOK

The presented analysis outlines the strategy of the energy management of the European XFEL, which covers 24 of the 26 1.3 GHz RF stations. It seems feasible to aim for "next shot" compensation of RF issues in Linac 3 even without magnet rescaling. Since the required quadrupole field changes are typically on the order of a few percent we could think of advanced corrections were the RF compensation is done immediately and the magnets following ignoring hysteresis effects. Such an approach would in general result in a lower optics mismatch than presented in Fig. 6. If hysteresis effects are critical the conclusion would be to use a reserve RF station at the end of Linac 3. In such a situation all field changes go in the same direction (compare Fig. 3) which by

ISBN 978-3-95450-133-5

using the correct branch of the hysteresis curve avoids field ambiguities. This investigation needs to be completed by an detailed look on how beam mismatch impacts the FEL performance.

An simple technique to stabilize compression was presented. Although magnet rescaling is required in case of Linac 2 RF problems. We will investigate more detailed compression fall-back scenarios including phase corrections in RF stations upstream of Linac 2.

A reliable automatized implementation of these procedures can even be used for temporary RF trips which are typically recovered on the order of minutes. Even thou this studies were conducted with the European XFEL in mind the basic principles are applicable for other facilities as well.

ACKNOWLEDGMENT

I would like to acknowledge helpful discussions and contributions from Winfried Decking, Martin Dohlus, Torsten Limberg, and Sascha Meykopff.

REFERENCES

[1] Massimo Altarelli et al., "The European X-Ray Free-Electron Laser Technical design report", DESY 2006-097, DESY, Hamburg, 2007

[2] W. Decking and T. Limberg, "European XFEL Post-TDR Description", XFEL.EU TN-2013-004-01, Hamburg, 2013

[3] H. Weise, "How To Produce 100 Superconducting Modules for the European XFEL in Collaboration and with Industry", Proceedings of IPAC2014, Dresden, 2014, WEIB03

[4] Yauhen Kot, Torsten Limberg and Igor Zagorodnov, "Different Charges in the Same Bunch Train at the European XFEL", DESY 13-215, Hamburg, 2013

[5] Igor Zagorodnov and Martin Dohlus, "Semianalytical modeling of multistage bunch compression with collective effects", Phys. Rev. ST Accel. Beams 14, 014403 – Published 13 January 2011

[6] Martin Dohlus, private communication.

ISBN 978-3-95450-133-5